



BIDIRECTIONAL AC-DC CONVERTER FOR REGENERATIVE BRAKING

Predrag Pejović¹, Johann W. Kolar², and Yasuyuki Nishida³

¹Faculty of Electrical Engineering, University of Belgrade, Serbia

²Swiss Federal Institute of Technology, Zürich, Switzerland

³Chiba Institute of Technology, Japan

Abstract: In this paper, a bidirectional AC-DC converter is analyzed. The converter applies a half-bridge thyristor rectifier and a recuperating thyristor bridge instead of a braking resistor. Recuperating mode of the converter is focused in the analysis, and it is shown that the converter exposes two operating modes within the recuperating mode, one characterized by negligible, and the other one characterized by significant distortion of the input voltages. Theoretical results are experimentally verified on a 10 kW converter.

Key Words: AC-DC power conversion, braking, converters, inverters, motor drives, phase control.

1. INTRODUCTION

In this paper, a half-bridge three-phase thyristor rectifier intended for application in machine drives, presented in Fig. 1, is analyzed. In many applications, like crane [1] or elevator drives, a machine drive that presents the load operates in generating mode, and the generated energy requires to be taken care of. One method to do this is to dissipate the generated power on a pulse width modulated braking resistor ([2], page 421). This method is reliable, simple, and robust, but requires additional cooling effort, significantly reduces the converter power density, and increases the energy cost. To avoid these drawbacks, bidirectional power converters are of interest. Full-bridge thyristor rectifiers are simple and robust, and provide bidirectional power flow, but in the inverting mode the output voltage has to be reversed [3], [4]. Refinements of this approach can be found in [5], [6], and [7]. To keep the voltage polarity in the inverter mode, auxiliary thyristor bridge accompanied by a free-wheeling diode (Fig. 1) is

proposed to replace the braking resistor voltage by the highest of the line voltages available at given time instant [8], [9]. Results presented in this paper are an extension of the results presented in [8] and [9], in theoretical direction, with the converter control and operating modes subjected to detailed analysis.

2. NOTATION AND NORMALIZATION

Let us assume that the converter is supplied by an undistorted symmetrical three-phase voltage system

$$v_k = V_m \cos\left(\omega t - (k-1)\frac{2\pi}{3}\right) \quad (1)$$

for $k \in \{1, 2, 3\}$. The supply lines are assumed to have leakage inductance L per phase, connected in series to the ideal voltage sources v_1 , v_2 , and v_3 . To simplify the notation, let us introduce two waveforms, one of them being the waveform of the voltage equal to the maximum of the phase voltages,

$$v_A = \max(v_1, v_2, v_3) \quad (2)$$

while the other one being the waveform of the voltage equal to the minimum of the phase voltages,

$$v_B = \min(v_1, v_2, v_3). \quad (3)$$

Since the phase voltages add up to zero,

$$v_1 + v_2 + v_3 = 0 \quad (4)$$

waveform of the voltage defined to be equal to the phase voltage that is neither minimal nor maximal at a considered time point can be obtained as

$$v_C = -v_A - v_B. \quad (5)$$

According to the definitions of v_A , v_B , and v_C , phase angle segments over the line period could be identified where indices of the phase voltages that represent v_A , v_B , and v_C do not change. There are six such segments, and they are given in Table 1. Table 1 also contains values of the index variables A , B , and C . For example, consider maximum of the line voltages $v_{AB} = v_A - v_B$ on the segment $\pi/3 < \omega t < 2\pi/3$; in that segment, $v_{AB} = v_2 - v_3$, since $A = 2$ and $B = 3$ over the segment. Besides the values of the phase voltage index variables, Table 1 also contains values of semiconductor index

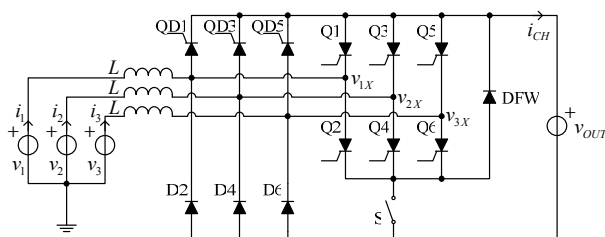


Fig. 1. The converter.

Table 1. Definitions of index variables A, B, C, a , and b .

range	A	B	C	a	b
$0 < \omega t < \pi/3$	1	3	2	1	6
$\pi/3 < \omega t < 2\pi/3$	2	3	1	3	6
$2\pi/3 < \omega t < \pi$	2	1	3	3	2
$\pi < \omega t < 4\pi/3$	3	1	2	5	2
$4\pi/3 < \omega t < 5\pi/3$	3	2	1	5	4
$5\pi/3 < \omega t < 2\pi$	1	2	3	1	4

variables a and b , where a is the index of the semiconductor component connected to the highest of the phase voltages, while b is the index of the of the semiconductor component connected to the lowest of the phase voltages.

Since numerical methods were extensively used to provide the results presented in this paper, to generalize the results normalization of variables is introduced. The voltages are normalized taking amplitude of the phase voltage as a basis, providing normalized value m_X of the voltage v_X as

$$m_X = \frac{v_X}{V_m}. \quad (6)$$

The currents are normalized taking amplitude of the short-circuit phase current as a base current for normalization

$$j_X = \frac{\omega L}{V_m} i_X. \quad (7)$$

The base current for normalization is high, thus all the currents in the analysis would be characterized by relatively low per unit values. For example, the RMS value of the phase short-circuit current is

$$I_{SC\,RMS} = \frac{1}{\sqrt{2}} \frac{V_m}{\omega L} \approx 0.707 \text{ p.u.} \quad (8)$$

A consequence is that the powers in the system would also be characterized by low per unit quantities, thus the short circuit apparent power is

$$S_{SC} = \frac{3}{2} \frac{V_m^2}{\omega L} = 1.5 \text{ p.u.} \quad (9)$$

Applying normalization defined by (6) and (7), the equation that characterizes the line inductance

$$v_L = L \frac{d i_L}{d t} \quad (10)$$

in normalized terms becomes

$$m_L = \frac{d j_L}{d \omega t}. \quad (11)$$

In analyses that follow, time variable t will be frequently represented by the phase angle variable ωt , like it has already been done in (11).

3. ANALYSIS OF THE CONVERTER OPERATION

Fundamental idea discussed in this paper is how to replace the voltage across the braking resistor with the maximum of the line voltages, v_{AB} , obtained applying the recuperating thyristor bridge of Fig. 1? Besides the voltage v_{AB} , the recuperating thyristor bridge provides connection to two L inductors that represent the line

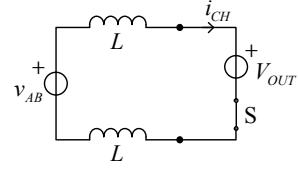


Fig. 2. Equivalent circuit of the converter during the recuperation interval.

inductance, connected in series to v_{AB} , as depicted in Fig. 2. In the analysis, it is assumed that the output voltage is constant. Thus, the output of the converter, including the output capacitor, is replaced by a constant voltage source V_{OUT} in the circuit diagram of Fig. 1, being supplied by the charging current i_{CH} , as depicted in Fig. 2.

According to the phase voltages (1), on the phase angle segment $0 < \omega t < \pi/3$ maximum of the line voltages is given by its normalized value

$$m_{AB}(\omega t) = \sqrt{3} \sin\left(\omega t + \frac{\pi}{3}\right) \quad (12)$$

reaching the minimum of $m_{AB}(0) = m_{AB}(\pi/3) = 1.5$. Now, let us assume that in the phase angle interval $0 < \omega t < \alpha$ the breaking switch of Fig. 1 is on, and that $M_{OUT} > m_{AB}$, which results in the recuperation interval. During the interval, normalized equation that characterizes the charging current is

$$\frac{d j_{CH}}{d \omega t} = \frac{1}{2} (m_{AB} - M_{OUT}). \quad (13)$$

Assuming that $j_{CH}(0) = 0$, the waveform of j_{CH} is given by

$$j_{CH}(\omega t) = -\frac{1}{2} \left(\sqrt{3} \cos\left(\omega t + \frac{\pi}{3}\right) + M_{OUT} \omega t - \frac{\sqrt{3}}{2} \right) \quad (14)$$

which for $M_{OUT} > \sqrt{3}$ reaches maximum of its magnitude for $\omega t = \alpha$, $j_{MAX} = -j_{CH}(\alpha)$.

Average of the charging current is computed performing averaging over the phase angle of $\pi/3$, which is the phase angle interval that corresponds to the fundamental period of the charging current,

$$J_{CH} = \frac{3}{\pi} \int_0^\alpha j_{CH}(\omega t) d \omega t \quad (15)$$

resulting in

$$J_{CH} = \frac{3}{4\pi} \left(2\sqrt{3} \sin\left(\alpha + \frac{\pi}{3}\right) + M_{OUT} \alpha^2 - \sqrt{3} \alpha - 3 \right). \quad (16)$$

In steady state, the converter output current is equal to the average of the charging current, $J_{OUT} = J_{CH}$, according to the charge balance over the filtering capacitor connected in parallel to the load. This is not shown in Fig. 1, but being assumed.

The charging current (16) is negative, which corresponds to the converter operation in the inverting mode. Normalized power in the inverting mode is given by $P_{OUT} = M_{OUT} J_{CH}$, and for various values of M_{OUT} and α it is depicted in Fig. 3. From the curves of Fig. 3 it can be observed that relatively high power could be recuperated, and that the process could be controlled

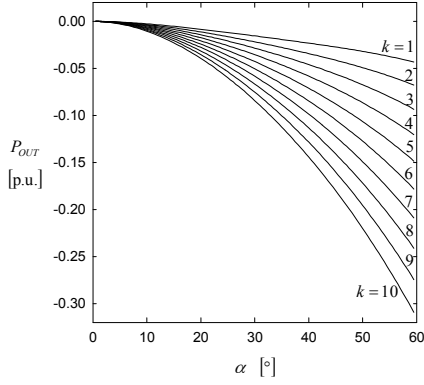


Fig. 3. Dependence of P_{OUT} on α for $M_{OUT} = 1.7 + 0.05k$.
varying the switch on-angle α , being also dependent on the converter output voltage.

Averaged equation over the output capacitor voltage governs the converter output voltage, and in normalized form it is given by

$$\frac{d m_{OUT}}{d \omega t} = j_{CH}(m_{OUT}, \alpha) - j_{OUT} . \quad (17)$$

Thus, dynamics of the converter in the recuperation mode is given by the first order nonlinear differential equation.

The analysis performed this far covers only the recuperating interval. However, at the end of the interval substantial amount of energy might remain stored in the inductors of Fig. 2. For example, for $M_{OUT} > \sqrt{3}$ the maximum of $|i_{CH}|$ flows through the inductors at the time instant when S is being turned off. This energy will be discharged through the free-wheeling diode (DFW in Fig. 1) during the discharge interval that follows the recuperating interval. Equivalent circuit for this interval corresponds to the circuit diagram of Fig. 2 with V_{OUT} replaced by a short circuit, and the governing equation for the current of the inductors i_L is

$$\frac{d j_L}{d \omega t} = \frac{1}{2} m_{AB} \quad (18)$$

where i_L is oriented in the same direction as i_{CH} . This interval lasts while $i_L < 0$. The discharge interval does

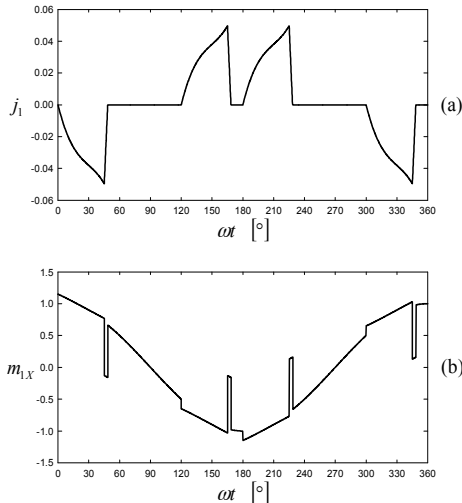


Fig. 4. Waveforms of j_1 and $m_{1,X}$ for $M_{OUT} = 1.8$ and $\alpha = 45^\circ$.

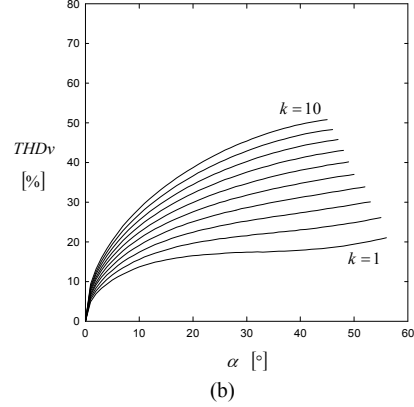
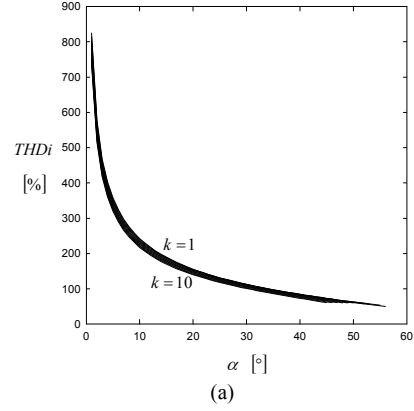


Fig. 5. Dependence of the input current (a) and the coupling point voltage (b) THD on α for

$$M_{OUT} = 1.7 + 0.05k .$$

not contribute to the recuperated power, since the voltage source that represents the load, is open during the interval. Typical waveforms of j_1 and $m_{1,X}$ in the recuperating mode are shown in Fig. 4.

Dependence of the input current THD and the THD of the voltages at the converter coupling points, just after the inductors that represent leakage inductances of the line, are presented in Fig. 5. The converter is characterized by high distortions of the currents and voltages, which might not be a fact of relevance in isolated local networks.

4. CONTROL OF THE CONVERTER

In the analysis presented this far, it was shown that the output voltage could be controlled adjusting the switch on angle α , and that the governing equation is a nonlinear first order differential equation (17). In this section, the analysis is extended to the output voltage below $M_{OUT} = \sqrt{3}$, down to $M_{OUT} = 1.5$, which is the bottom limit to turn the thyristors Q1 to Q6 on. In this case, the charging current i_{CH} may reach zero spontaneously, causing the thyristors of the recuperating bridge to turn off, without any need for hard switched turn off of S. This operating mode is named soft discharge mode.

According to (13), at low output voltages, lower than $\sqrt{3}$ p.u. , recuperating current grows in magnitude as long as $m_{AB} < M_{OUT}$, while it starts to decrease when $m_{AB} > M_{OUT}$. For the output voltages lower than about 1.67 p.u. , the recuperating current reaches to zero during the recuperating interval, and the thyristors Qa and Qb

turn off spontaneously. Exact limit of this operating mode is $M_{OUT} < M_{SDM}$, where M_{SDM} is obtained as a solution of

$$M_{SDM} \arcsin \frac{M_{SDM}}{\sqrt{3}} + \sqrt{3 - M_{SDM}^2} - \frac{2\pi}{3} M_{SDM} + \frac{\sqrt{3}}{2} = 0. \quad (19)$$

Numerical solution of (19) is $M_{SDM} \approx 1.673436$. In the case $M_{OUT} < M_{SDM}$, the line inductance discharge is spontaneously performed. In this manner, the voltage spikes related to the discharge process after the hard turn off of S are avoided, and the THD of the input voltages remains moderate. In the first two diagrams of Fig. 6, the input current and the input voltage are presented for the converter operating in this mode, at $M_{OUT} = 1.65$ and $\alpha = 45^\circ$, corresponding to $J_{OUT} = -0.023$. The THD of the input current, presented in Fig. 6(a), was expectedly high, equal to 127%. However, the THD of the input voltage waveform, presented in Fig. 6(b), was only 2.73%, which is a consequence of the absence of the voltage spikes that characterize the discharge process caused by hard turn off of S. Applying numerically

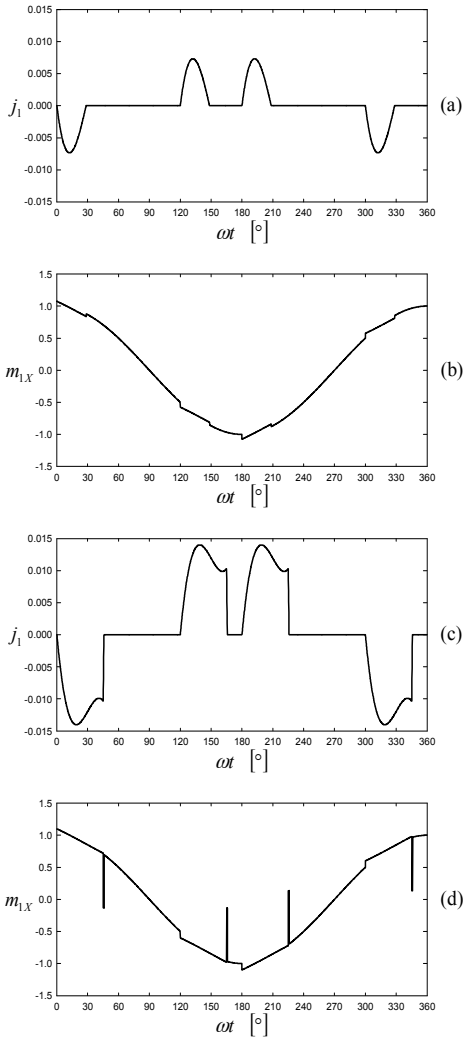


Fig. 6. Waveforms of the input current and the input voltage for $\alpha = 45^\circ$: (a) and (b) soft discharge mode at $M_{OUT} = 1.65$; (c) and (d) hard discharge mode at $M_{OUT} = 1.7$.

obtained value for M_{SDM} , maximum of the recuperated current absolute value in the soft discharge mode is obtained as $J_{OUT} = -0.004291$, which corresponds to the recuperated power of $P_{OUT} = -0.007181$ p.u., or in the terms of the short circuit apparent power at the point of coupling

$$\frac{P_{OUT}}{S_{SC}} = -0.4787\%. \quad (20)$$

Output current of recuperating mode increased above the soft discharge limit forces the converter to operate in the hard discharge mode. The input current and the input voltage waveforms that correspond to this operating mode at $M_{OUT} = 1.7$ and $\alpha = 45^\circ$, corresponding to $J_{OUT} = -0.0081$, are presented in the last two diagrams of Fig. 6, labeled (c) and (d). The THD of the input current is reduced to 69.44%, while the THD of the input voltage is increased to 11.77%.

In order to compare the converter behavior in the soft discharge mode to the operation in the hard discharge mode, a set of numerical simulations is performed. In Fig. 7(a) dependence of the recuperated current J_{OUT} on the output voltage M_{OUT} is presented. It can be observed that for normalized output voltages lower than M_{SDM} absolute value of the recuperated output current is relatively low in magnitude, lower than the limit of 0.00429 p.u. Increased output voltage causes the converter to operate in the hard discharge mode, resulting in increased absolute value of the recuperated current. In Fig. 7(b), dependence of the input voltage THD on the output voltage is presented. Point where the converter switches from soft discharge mode to the hard

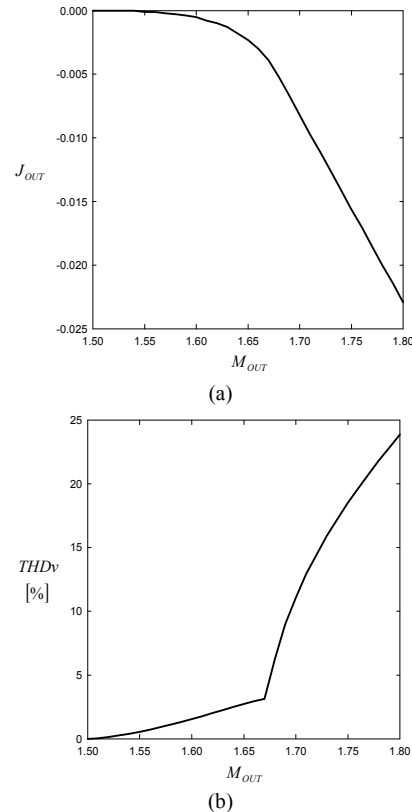


Fig. 7. (a) Dependence of J_{OUT} on M_{OUT} for $\alpha = 45^\circ$; (b) dependence of the input voltage THD on M_{OUT} for $\alpha = 45^\circ$.

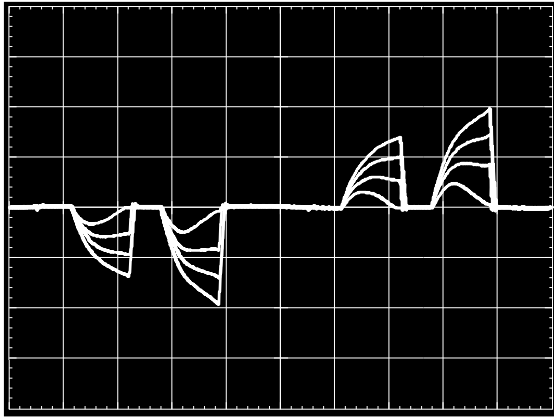


Fig. 8. Waveforms of the input current for the output voltages of 590 V, 580 V, 570 V, and 550 V. Scales: 20 A/div, 2 ms/div.

discharge mode is readily observable by sudden increase of the input voltage THD.

It can be concluded that the converter at low output voltages and relatively low recuperating power could be operated in the soft discharge mode, which is characterized by absence of the input voltage spikes and moderate distortions of the input voltages. Besides, hard switched turn off of S is avoided in this mode. In the case the load tolerates the output voltage variations of about 20%, it is possible to operate the converter with a constant on-angle of S. In that case, at higher recuperating power the converter would operate in the hard discharge mode, while at lower recuperating power the converter would operate in the soft discharge mode.

5. EXPERIMENTAL RESULTS

In order to verify feasibility of the proposed concept, a laboratory model of the converter with the rated power of 10 kW was built applying IXYS VVZB 120 module for the half controlled thyristor bridge and the controlled switch, and six discrete thyristors IXYS CS 30-12oi, for the recuperating thyristor bridge. The converter is intended to operate at the three-phase voltage system with the phase voltage RMS value of 230 V, at 50 Hz. The line inductance was 1 mH. The output voltage of the converter was impressed by an external DC source, which is applied to provide the power to be recuperated to the mains. To analyze the effects caused by the supplying three-phase voltage system unbalance, voltage at one of the phases is increased for about 4% by an adjustable transformer.

To illustrate the converter operation at different output voltages, while keeping the switch on-angle constant, a set of measurements is performed, and obtained waveforms of the input currents are presented in Fig. 8. The measurements are performed for four values of the output voltage: 590 V, 580 V, 570 V, and 550 V. These output voltages correspond to the recuperating power of 9.3 kW, 7.2 kW, 5.4 kW, and 1.6 kW, respectively. Operation of the converter in the soft discharge mode at the lowest of the power is clearly observable.

6. CONCLUSIONS

In this paper, a bidirectional AC-DC converter intended for application in machine drives to provide

regenerative braking is analyzed. The converter is derived replacing the braking resistor by a thyristor bridge that provides the maximum of the line voltages at its output in order to recuperate the braking energy. Appropriate normalization is introduced to generalize the results. Operation of the converter is analyzed in detail, and it is shown that the converter in the recuperating mode can operate in two sub-modes: soft discharge mode and the hard discharge mode. The soft discharge mode is shown to provide recuperation with negligible distortion of the input voltages. Limits for this operating mode are derived. Constant on-angle control strategy for the recuperating switch is analyzed, and it is shown to be applicable for the loads that tolerate 20% variation of the supply voltage. The analyses are experimentally verified on a 10 kW converter laboratory model.

7. REFERENCES

- [1] R. Belmans, F. Busschots, R. Timmer, "Practical design considerations for braking problems in overhead crane drives," in IEEE Industry Applications Society Annual Meeting, 1993, pp. 473-479.
- [2] N. Mohan, T. M. Undeland, W. P. Robbins, *Power Electronics: Converters, Applications and Design*, 2nd Edition. New York: John Wiley & Sons, 1995.
- [3] R. M. Davis, "A bidirectional AC-DC power converter for fixed polarity DC loads," in 3rd International Conference on Power Electronics and Variable Speed Drives, London, UK, 1988, pp. 142-145.
- [4] D. Milly, "An AC to DC converter with output reversion," in Record of the 3rd European Conference on Power Electronics and Applications, Aachen, Germany, 1989, pp. 813-817.
- [5] J. C. Clare, P. R. Mayes, W.F. Ray, "Bidirectional power converter for voltage fed inverter machine drives," in 23rd Annual IEEE Power Electronics Specialists Conference Record, 1992, pp. 189-194.
- [6] K. Matsui, K. Tsuboi, S. Muto, "Power regenerative controls by utilizing thyristor rectifier of voltage source inverter," IEEE Transactions on Industry Applications, vol. 28, pp. 816-823, July/Aug. 1992.
- [7] K. Matsui, U. Mizuno, Y. Murai, "Improved power regenerative controls by using thyristor rectifier bridge of voltage source inverter and a switching transistor," IEEE Transactions on Industry Applications, vol. 28, pp. 1010-1016, Sep./Oct. 1992.
- [8] J. W. Kolar, H. Ertl, F. C. Zach, "A novel concept for regenerative braking of PWM-VSI drives employing a loss-free braking resistor," in 12th Annual Applied Power Electronics Conference and Exposition APEC '97 Conference Proceedings, 1997, pp. 297-305.
- [9] J. W. Kolar, H. Ertl, F. C. Zach, "Design and experimental evaluation of the loss-free braking resistor concept for applications in integrated converter machine systems," in Proceedings of the 24th Annual Conference of the IEEE Industrial Electronics Society, IECON '98, 1998, pp. 626-629.